APPENDIX A - EXPERIMENTAL PROCEDURE

A.1 Background to Experimental Plan

Prior to the initiation of the experimental phase of the project, a review of recent literature describing the methodologies and instrumentation employed in similar crash experiments was undertaken. Particular attention was focused on work carried out at Battelle Columbus laboratories and Wayne State University.

In August 1979, the principal investigator in this study visited the researchers at Battelle's Columbus laboratories, Wayne State University and the Traffic Research Centre, Ohio to gain first-hand information on the conduct of controlled full-scale vehicle-pedestrian collisions.

Preparation for the crash experiments commenced in December 1979. The first full-scale collision was executed in early February 1980 with the Gemini coupe. The first crash experiment with the HZ sedan was carried out in early March 1980. The final data-gathering experiment was completed in the same month.

A.2 Test Area and Vehicle Preparation

The vehicle-pedestrian impact tests were conducted at a test track on the RMIT campus. The track is long enough to accommodate a production vehicle impacting an adult pedestrian dummy at a maximum speed of 25 km/h. The test site is 60 metres long and 6 metres wide at the narrowest part and 12 metres wide at the broadest (Fig. A1). A grey backdrop was erected to effect a contrasting background for the experiments. Fig. A2 shows the test site during one of the experiments. The vehiclesacquired for the experiments were a prototype Gemini coupe and a 1978 Holden HZ sedan. Windscreen guards were fitted to both vehicles to prevent possible penetration into the passenger compartment during the tests. The vehicleswere driven by the same driver in each run. Prior to each set of experiments, the driver was carefully drilled to achieve a consistent impact speed and

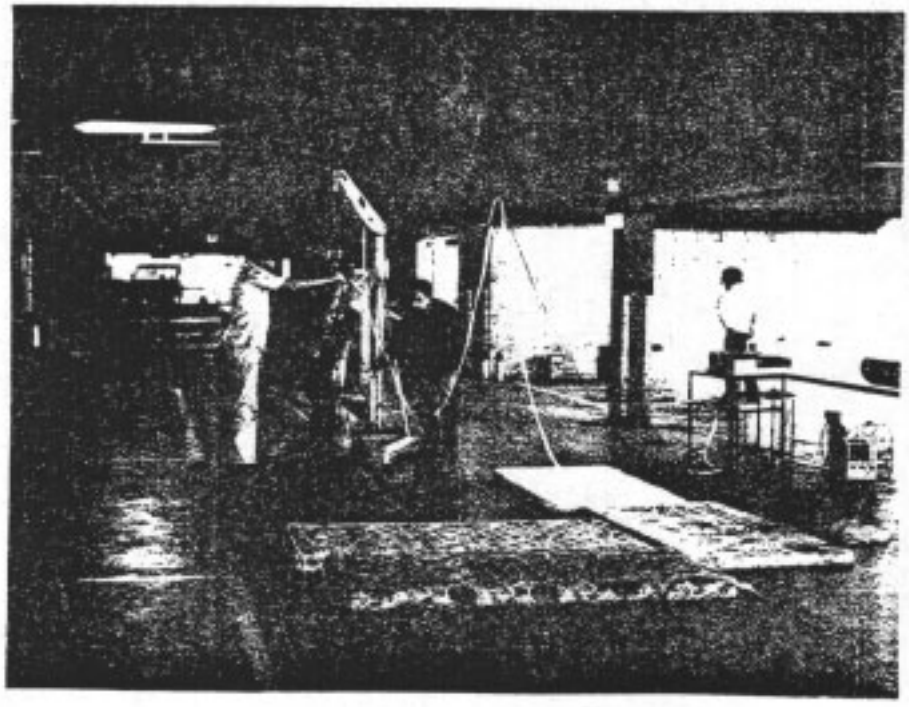

FIGURE A.1 Test site at RMIT

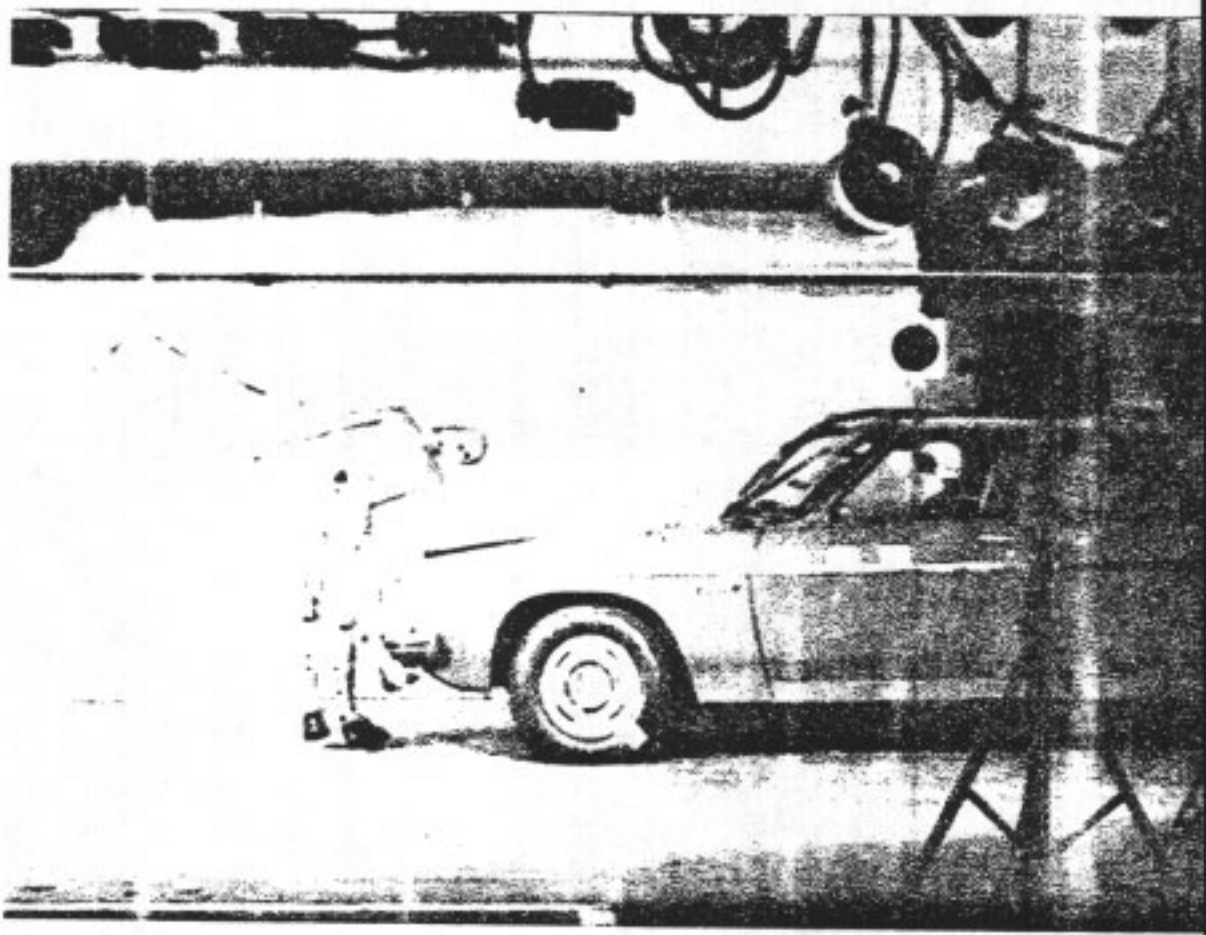

braking response. These driver associated variables were carefully checked after each experiment.

An impact speed of 20 km/h was selected for all tests. This value was partly dictated by inexperience with the resistance of the pedestrian dummy to impact. The speed of 20 km/h has been used as the lower limit in most pedestrian tests overseas and is considered as an upper limit in 50% of car-pedestrian accidents in urban areas in Germany (Erke, 1975).

A.3 Test Subject Preparation

The test subject is a fifty percent adult anthropometric dummy from Humanoid Systems, Inc. (Fig. A3). The dummy possesses free-standing ability, with approximate equal weight distribution on each foot.

FIGURE A.3 50% Adult anthropometric pedestrian dummy

All the impact experiments were carried out with the dummy in a walking position facing in the direction perpendicular to the pat of the vehicle. The position of initial impact was maintained at the front left side of the vehicle, i.e. approximately 300 mm from the vehicle's longitudinal axis. This configuration simulat the most common mode of collision where the pedestrian walks onto the road and is impacted on his right side by the left front half the car. It has been found in 93% of car-pedestrian collisions i Germany (Matthoefer, 1976).

Impact tests using the Gemini were carried out with the dummy ful dressed. Foam padding was used on the ground to reduce possible damage to the dummy during the secondary impact. This protective measure was dictated by the inexperience with the dummy and by th information about pedestrian tests at Battelle, Ohio (Pritz, 1977 where special tethering for dummy protection was used.

Results from the Gemini tests showed that a dressed dummy could n display clearly the motion of its limbs and that the secondary im with the road would not damage the dummy for the exercised vehicl speed of 20 km/h.

Subsequent experiments with the large car were therefore conducted without any clothing (except shoes) and without foam padding on the roadway.

All limb joints, except the ankles which were locked to enable fre standing, were pre-set at a torque allowing free motion at accelerations of about 1 g. This setting permits simulation of th loss of muscular control of the limbs during the impact phase and in accordance with international practice in pedestrian safety research. During the initial experiments with the Gemini, the right ankle of the dummy fractured on impact with the thermoplasti bull-bar. After stiffening the right ankle the right knee was fractured (Fig. 5.1 . The right knee was then stiffened. In the n experiment with a steel bull-bar the left ankle was broken.

Stiffened joints were used in subsequent HZ Sedan tests to save on repair time. Comparison of dummy motion in the Gemini and the HZ Sedan tests clearly shows that dummy's right ankle and/or right knee would have fractured in all the HZ Sedan tests with bull bars fitted to the car.

A.4 Instrumentation

A.4.1 Photography

One high speed camera was used to film the entire lateral sequence of the primary impact. A motor-driven 35 mm camera, placed in front of the impact site provided transverse coverage of the collision. Details of the photographic instrumentation are presented in Table A.1

TABLE A.1 PHOTOGRAPHIC INSTRUMENTATION

Camera	Lens	Distance (m)	Film Type	Frame Speed
Hycam	15 mm	7	Kodak Ectachrome 7250 colour	500 p.p.s.
Nikon	50 mm	20	Kodak TRI-X ASA 400 B & W	3 p.p.s.

A timing light in the Hycam high-speed camera placed a mark on the edge of the film at 10 millisecond intervals.

Targets were placed against the grey backdrop and on the side panels of the vehicles to facilitate analysing film of the impacts. These 100 mm x 50 mm rectangular targets provide a fixed reference for the instanteous position of the vehicle. Alternately black and yellow targets, each 20 mm square were placed on the head, torso and the limbs of the dummy to determine its instantaneous position and orientation during the impact phase.

Twenty-six quartz-iodine lamps, each dissipating 1 kW, were used to illuminate the test track for the experiments (Fig. A.2) An aggregate of 27 kW was required to operate all the instrumentation for the experiments.

A.4.2 Accelerometers

A total of two triaxial and four uniaxial piezoelectric accelerometers yielding ten channels of data were used for the experiments. The accelerometers were fastened onto brackets and bolted on the respective parts of the body. Table A.2 provides details of the individual accelerometers utilised in the tests.

TABLE A.2 DETAILS OF PIEZOELECTRIC ACCELEROMETERS

Accelerometer	Type	Location	Max g/level (g)	Flat Frequency Range (kHz)	Overall Sensiti (mV/s)
B & K 4321	Triaxial	Head	1000	8	9.62
	Triaxial	Pelvis	1000	8	9.62
B & K 4332	Uniaxial	Knee	6000	15	10
	Uniaxial	Knee	6000	15	10
	Uniaxial	Knee	6000	15	10
B & K 4338	Uniaxial	Foot	1000	3	9.62

A.4.3 Amplifiers

Charge preamplifiers were selected over the voltage amplifiers because of the necessity of using long accelerometer cables and t inherently lower limiting frequency of the former. Two models of charge preamplifiers were used. The specifications and details o the respective accelerometer-preamplifier coupling are presented table A.3.

TABLE A.3 DETAILS OF CHARGE AMPLIFIERS

Type	Quantity	Accelerometer	Lower Limiting Freque (Hz)
B & K 2634	3	B & K 4321 Head	1.0
B & K 2634	3	B & K 4321 Pelvis	1.0
B & K 2635	3	B & K 4332 Knee	0.2

A.4.4 Cables

The instrumentation cables comprised two segments. The transducers were connected to the preamplifiers by teflon-insulated low noise coaxial cables, specially treated to minimise tribo-electric noise at low frequencies. These cables, identified as transducer cables, are approximately 10 m long. The ten cables were taped together and suspended by cotten thread from the ceiling before each test. These cables were sufficiently light not to interfere with the pedestrian dynamics.

The second set of cables connected preamplifiers to the tape-recorders and are hence termed data cables. They are conventional single shielded high impedance coaxial cables each 1 m long.

Calibration of the system was achieved by means of an electrodynamic vibration platform which produces a reference acceleration level of 10 ms^{-2} (1.02 g). It should be noted that the calibration was accomplished with all instrumentation connected as in the actual experiment. This procedure eliminated the problems arising from cable impedance associated with long cable lengths. In addition, a reference calibration signal was recorded on tape for each channel. This serves as the reference level for subsequent data reproduction.

A.5 Data Recording and Processing

Two multi-channel instrumentation tape-recorders, giving an aggregate of 10 frequency modulated (FM) channels were utilised to record the signals. A single amplitude modulated (AM) channel was used for verbal comments. Data recording was carried out at the maximum tape speeds of 38 cm/s and 152 cm/s respectively. The impact data were filtered at 1 kHz and stored permanently as magnetic tape.

The data was analysed and processed with a Hewlett-Packard 5451C Fourier Analyser. The analogue data were digitized at a minimal rate of 9000 samples and stored at disc for easy accessibility.

Various analyses of the signals were accomplished, namely peak values of the resultant acceleration, the pulse duration, and th Gadd Severity Index.* The results were then displayed on a HP 26 visual display unit. Hard copies were obtained from a HP 9862A plotter connected to the analyser.

* See Appendix C

APPENDIX B - SIMPLE ANALYTICAL MODEL OF A PEDESTRIAN

The pedestrian is modelled as a rigid body with the centre of gravity in the point C having the mass m and moment of inertia J_C about C and resting on the road in the point B. He is hit by the car in the point A.

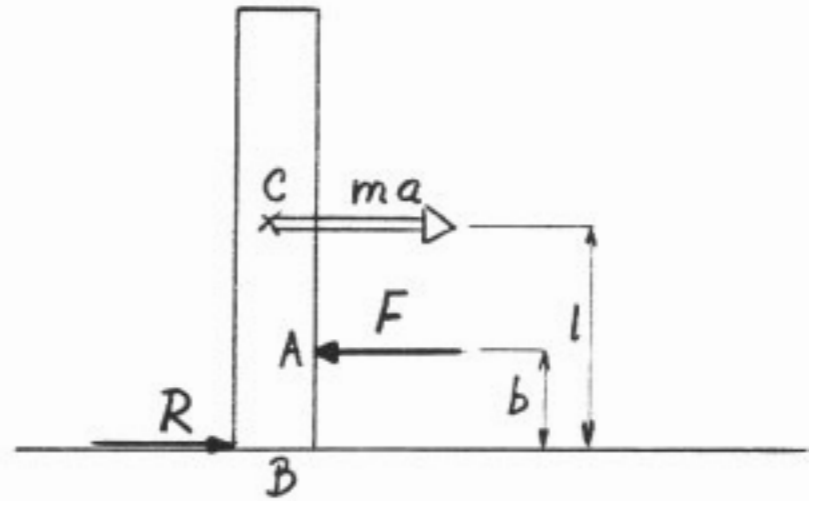

FIGURE B.1 A simple model of a pedestrian hit by a car

During the impact, a force F in the contact point A will accelerate the body with a linear acceleration a_C of C and angular acceleration α_C about C.

Assume first that the reaction force R in the contact area between the feet and the road is smaller than the friction force. The body will then rotate about the point B and the accelerations a_C and α_C will be coupled by the condition $a_C = \ell.\alpha_C$
The equations of motion of the body are

$$F - R = ma_C, \qquad \text{(B.1a)}$$

$$R.\ell - F(\ell - b) = J_C\alpha_C. \qquad \text{(B.1b)}$$

Excluding the accelerations a_c and α_c from the equations (B.1) give

$$R = F.(J_c+m\ell^2-m\ell b)/(J_c+m\ell^2) \qquad (B.2)$$

Assuming the unchanged bumper stiffness (F constant) and unchanged dummy properties (J_c, m, ℓ constant), the reaction R will increase with decreasing distance b as it is evident from the equation (B.2).

The maximum value the reaction R can reach is the friction force μW, where μ is the coefficient of friction between the feet and the road and $W = mg$ is the weight of the body.

To ensure that the friction force will be overcome, the distance b of the impact point from the road must satisfy the condition

$$b < (J_c+m\ell^2)-(F-\mu W)/m\ell F \qquad (B.3)$$

The body will then rotate about C.G. and the feet will be free from the road immediately after impact.

The model can also explain the importance of the bumper stiffness. By regrouping the variables the equation (B.3) can be written as

$$b < \frac{J_c+m\ell^2}{m\ell}\left(1-\frac{\mu W}{F}\right).$$

All other parameters remaining unchanged, a smaller force F requires a smaller value of b to overcome the friction force μW (see Fig.B.2).

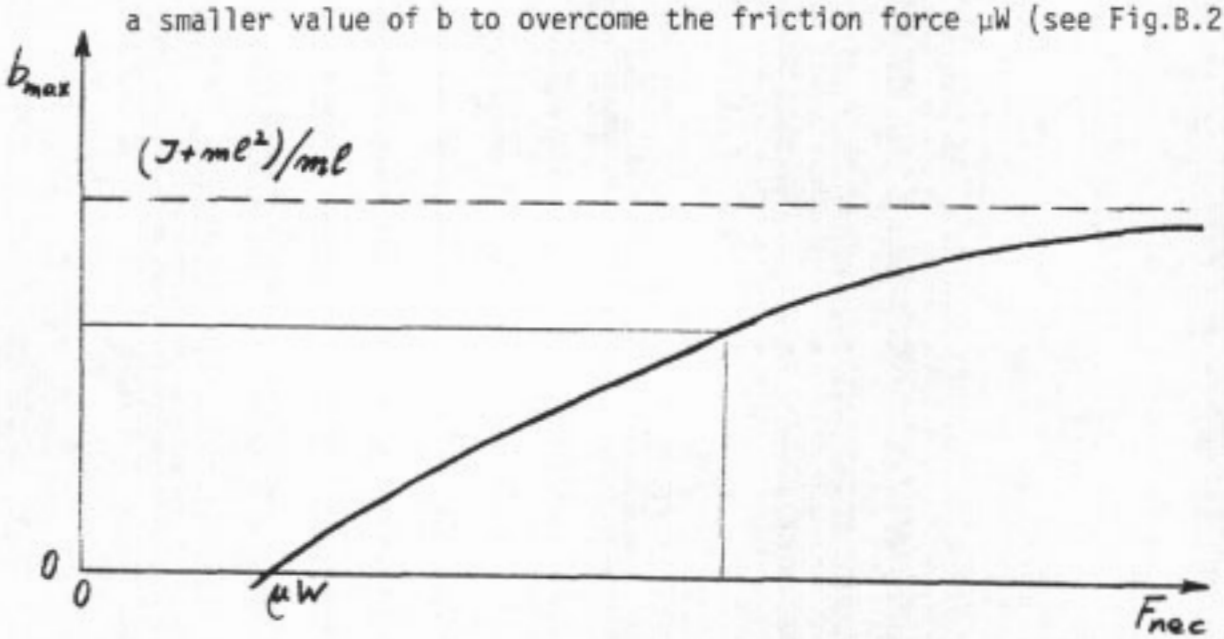

FIGURE B.2 Necessary impact force F_{nec} to overcome the friction for the given bumper-road distance b

It takes a finite time for the force F to reach the necessary value F_{nec} to initiate movement of the foot along the road surface. During this time, the foot will not move and the leg will rotate about the foot-road contact point. The longer it takes to reach the value F_{nec}, the further forward the upper leg will move with respect to the foot(Fig. B.3).

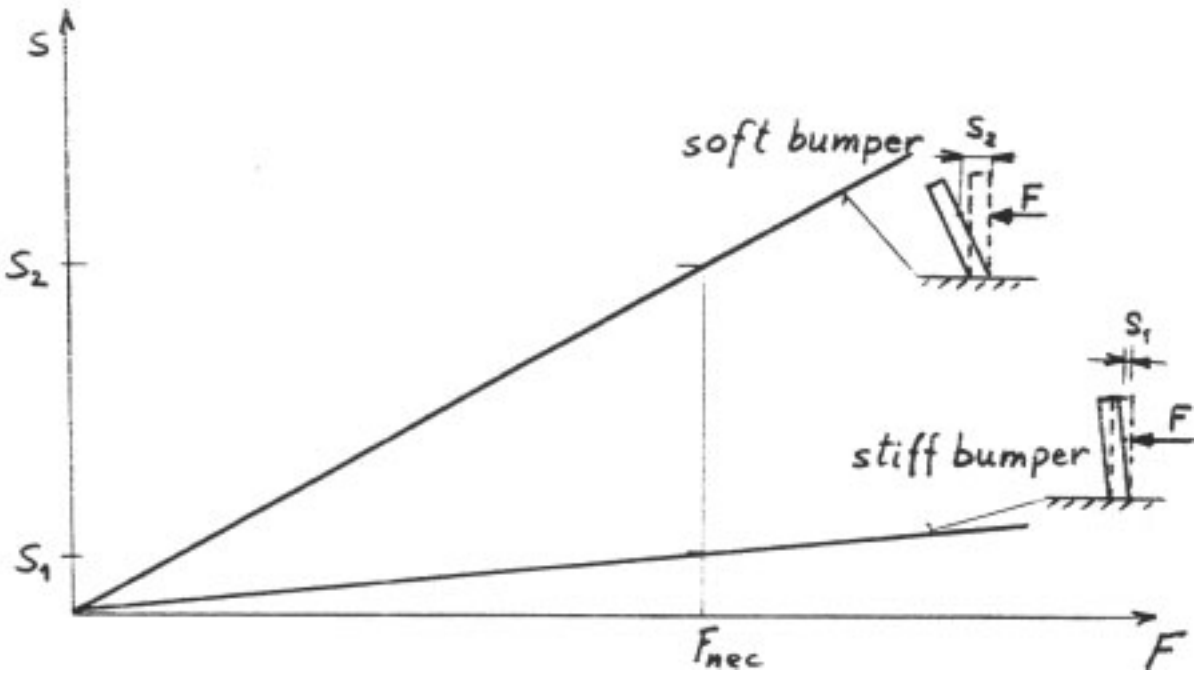

FIGURE B.3 Effect of the bumper stiffness on the leg position at the instant of sliding

A stage can be reached when the foot will be locked between the road and leg and the ankle and/or knee breaks as the pedestrian rotates over the bonnet.

APPENDIX C - INJURY CRITERIA

To obtain an absolute value of the degree of injury of a pedestrian in simulated car-pedestrian collisions is a difficult task. Tolerance of individuals to injury can widely change from person to person, the evaluation of the severity of many types of injury is a complex problem and the correlation of data measured on cadavers and dummies with the injury tolerance of living human bodies is still not well established.

Head Injury Criteria

The evaluation of head injury is the best established one. There are three accepted procedures used in engineering practice:

(a) Wayne State University Tolerance Limit (Fig. C.1)

It is based on experiments with animals and human cadavers. The WSU curve represents the threshold of injury. It is evident that the shorter the impact duration the higher acceleration can be tolerated.

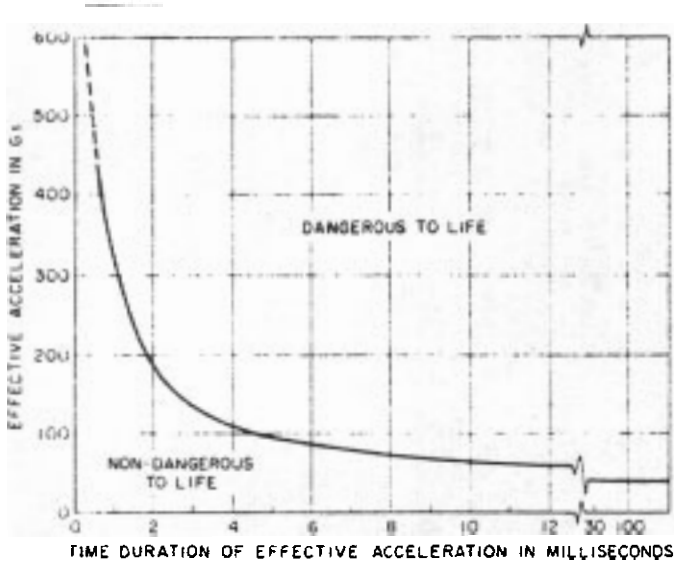

FIGURE C.1 Wayne State University Tolerance Limit

(b) SAE Severity Index (Gadd Severity Index)

The formula for the calculation of the Severity Index (SI) is defined by SAE J885 (28) Standard.

$$SI = \int_0^T \left(\frac{a}{g}\right)^{2.5} dt$$

where a is the absolute value of the resultant acceleration, T is the total time of the impact. The threshold for the injury is SI = 1000.

(c) Head Injury Criterion

Discrepancies between experimental results and the values of SI indeces indicated that the SI Index was too conservative in over estimating the peak values at short intervals. A better correlation is obtained by using HIC Index as defined by Versace 1971.

$$HIC = \max \quad \{(t_2 - t_1) \left[\frac{1}{t_2 - t_1} \int_{t_1}^{t_2} \right. \qquad (C.2)$$

where t_1 and t_2 ($t_2 > t_1$) are two parameters and the weighting by the coefficient 2.5 is applied to the mean value of the acceleration over the $t_2 - t_1$ internal. HIC value is the maximum value obtained by changing t_1 and t_2 over the time internal of the impact. The disadvantage of HIS is its laborious evaluation.

The HIC threshold for the injury is again set to 1000.

Other Injuries

The severity of injuries of other parts of the body is usually estimated by comparison with threshold values of acceleration and/or forces. These values have been obtained from experiments with cadavers and animals under static or dynamic conditions. Table C.1 shows some data as found from the literature (Matthofer, 1976).

TABLE C.1 SELECTED VALUES OF INJURY TOLERANCE

Head	a_{max}	100 .. 300 g
	WSU-curve	60 g at t > 45 ms
	SI-index	1000
	HIC-index	1000
Chest	a_{max}	40 .. 60 g, t > 3 ms > 60 g, t < 3 ms
	F_{max}	4000 .. 8000 N
	s_{max}	5 .. 6 cm
Pelvis	a_{max}	50 .. 80 g
Knee	F_{max}	6400 .. 12 500 N

APPENDIX D - EVALUATION OF PEDESTRIAN ACCELERATIONS (50% ADULT DUMMY AND HZ HOLDEN SEDAN)

Analysis of pedestrian injuries resulting from collisions with passenger cars at speeds of 40 km/h and less revealed that about two-thirds of non-minor injuries are caused by contact with the vehicle and one third by secondary impact with the road or roadside objects (Daniel, Eppinger, 1979). For adults, contact with the car is the main cause of pelvic (100%) and lower extremity (87%) injuries. The distribution of total injuries is about 30% head, 35% lower extremities, 10% pelvis.

The standards for estimation of head injury are well defined and are based on acceleration level (see Appendix C.) The criteria for leg injuries are based on force, bending moment and energy measurements. The limited time for the project did not allow the development of a reliable force measurement technique. Therefore the effect of bull-bar on leg injury is estimated on a comparative basis only.

Head (Fig. D1-D4)

There is no primary impact of the head with the car in each of the three cases when bull-bar has been attached (Fig. D2-D4). In the case without a bull-bar, the head struck the bonnet at 280 ms (Fig. D1). Periodic changes from 280 to 800 ms show slightly damped vibrations of the head on the elastic bonnet (about 10 g amplitude and 100 ms period or 10 Hz frequency). The severity is well below the threshold in WSU curve (about 15 g over 10 ms). Secondary impacts of the head with the road are clearly seen in all four cases. (Notice the different scales of accelerations.)

The peak value in the case without bull-bar is about 65 g at 1100 ms. The duration of the peak is not longer than 5 ms. Comparison with WSU curve (Fig. D5 point N1) shows that this value of acceleration is not dangerous.

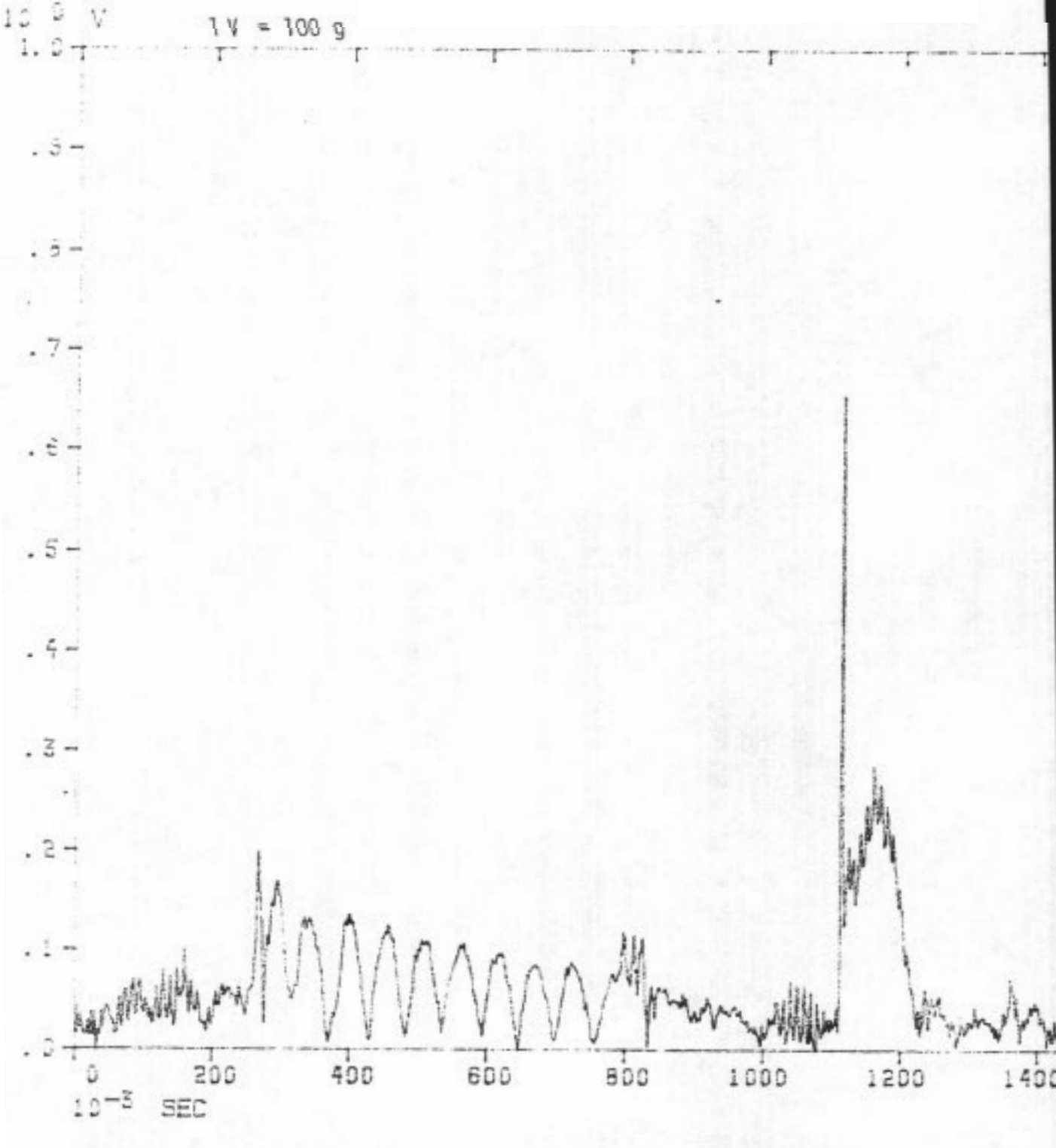

FIGURE D1 - Resultant head acceleration for HZ Sedan without a bull-bar

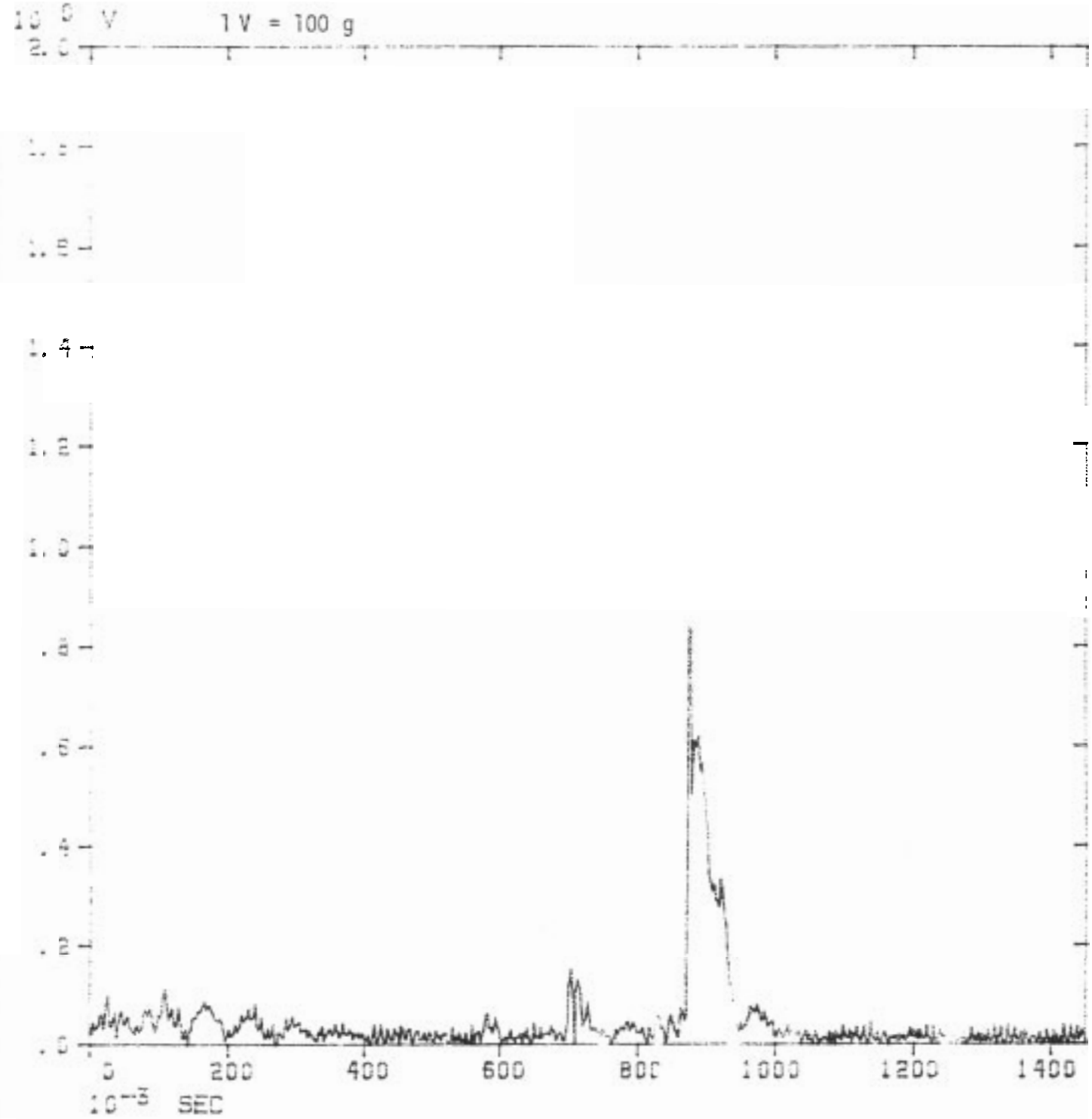

FIGURE D2 - Resultant head acceleration for HZ Sedan with an aluminium bull-bar

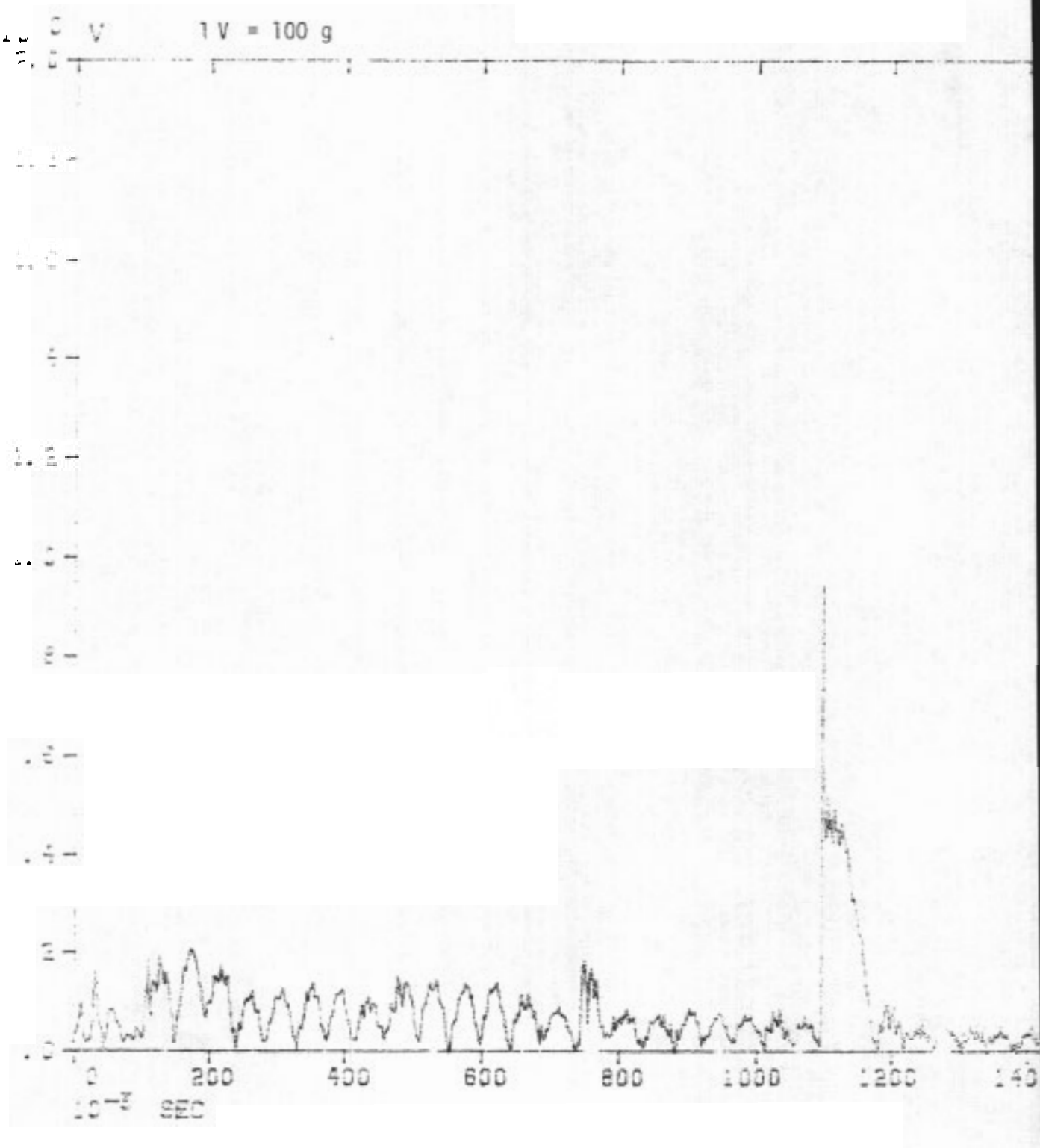

FIGURE D3 - Resultant head acceleration for HZ Sedan with a tubular steel bull-bar

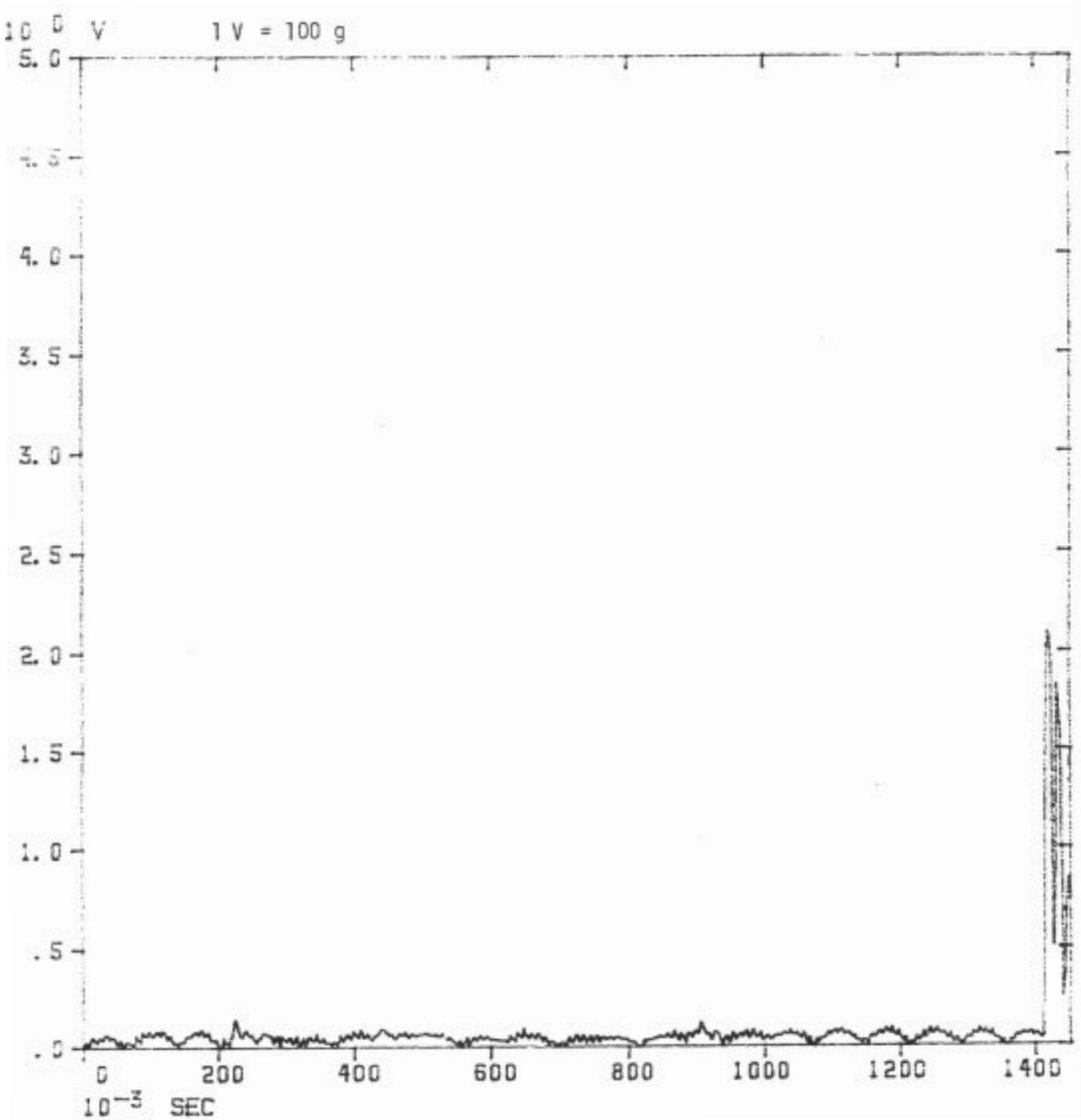

FIGURE D4 - Resultant head acceleration for HZ Sedan with a truck type bull-bar

Also the second peak (rebound) of 20 g over 100 ms (point N2 in (Fig. D5) is well below the threshold.

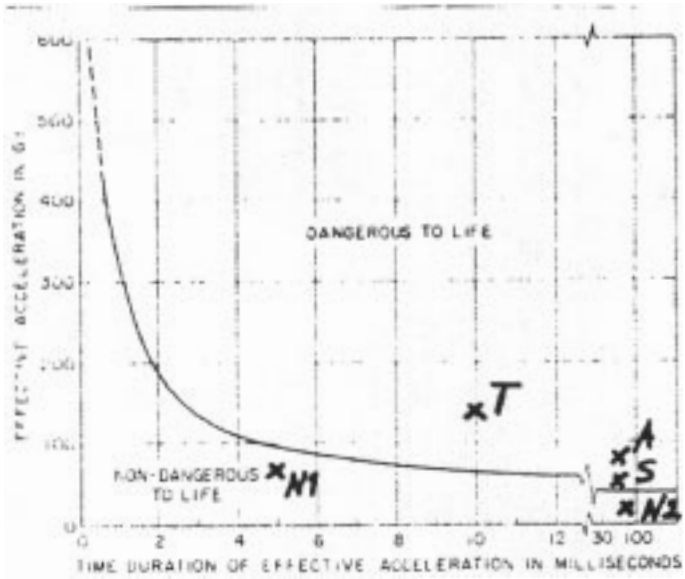

FIGURE D.5 Comparison of impact severity with WSU-curve
N-no bull-bar, S-tubular steel bull-bar
A-aluminium bull-bar, T-truck type bull-bar
Impact speed 20 km/h

The aluminium bull-bar causes a peak of 60 g over at least 30 ms which is above the threshold (point A in Fig. D5). The steel bull-bar (Fig. D3) results in a peak of about 45 g over a tim interval of at least 50 ms which is just above the threshold (points in Fig. D5). Largest values of head acceleration occur in the case of heavy truck bull-bar (Fig. D4). The duration of the value of 170 g is at least 10 ms which is substantially above the tolerance level (point T in Fig. D5).

A better evaluation of impact severity is achieved by calculation of severity indices. SI indices have been evaluated for each of the four cases using the formula C.1.

The values are (threshold 1000)

no bull bar	850
aluminium	1350
steel	1050
truck type	2350

Comparison with the points in Fig. D5 shows a similar result, i.e. the heavier the bull-bar the higher severity of head injury.

Knee (Fig. D6-D9)

As already mentioned, the evaluation of severity of leg injury cannot be based on absolute acceleration levels. Nonetheless, the recorded data can serve to demonstrate differences due to bull-bar mounting.

Fig. D7 and D8, showing knee accelerations for impact with aluminium and steel bull-bars, respectively, can be very well correlated to corresponding frames in Fig. 4.2.

The smooth signal reveals that there was no direct contact between the lower leg close to the knee and the bull-bar. In the case of the aluminium bar, the leg remained almost stationary during the whole impact (signal has been lost after 470 ms). The steel bull-bar locked the leg during first 120 ms but then the moment of the rotating upper torso managed to overcome the moment of the friction force due to the lower position of the upper bar as compared with the aluminium bull-bar.

The curves on Fig. D6 and D9 in the region of the secondary impact have an oscillatory character indicating that there was a direct impact into the leg close to the knee area.

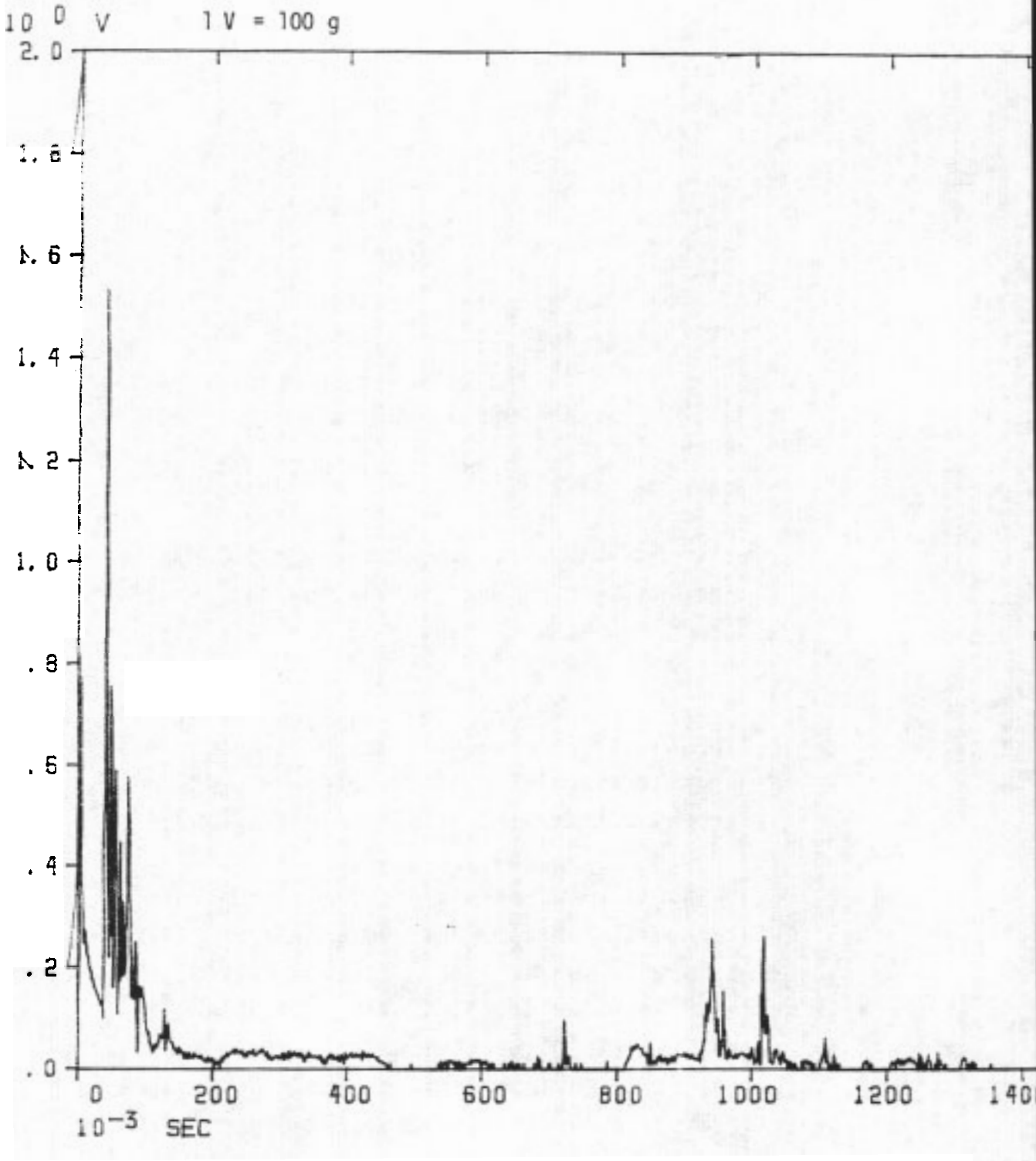

FIGURE D6 - Resultant knee acceleration for HZ Sedan without a bull-bar

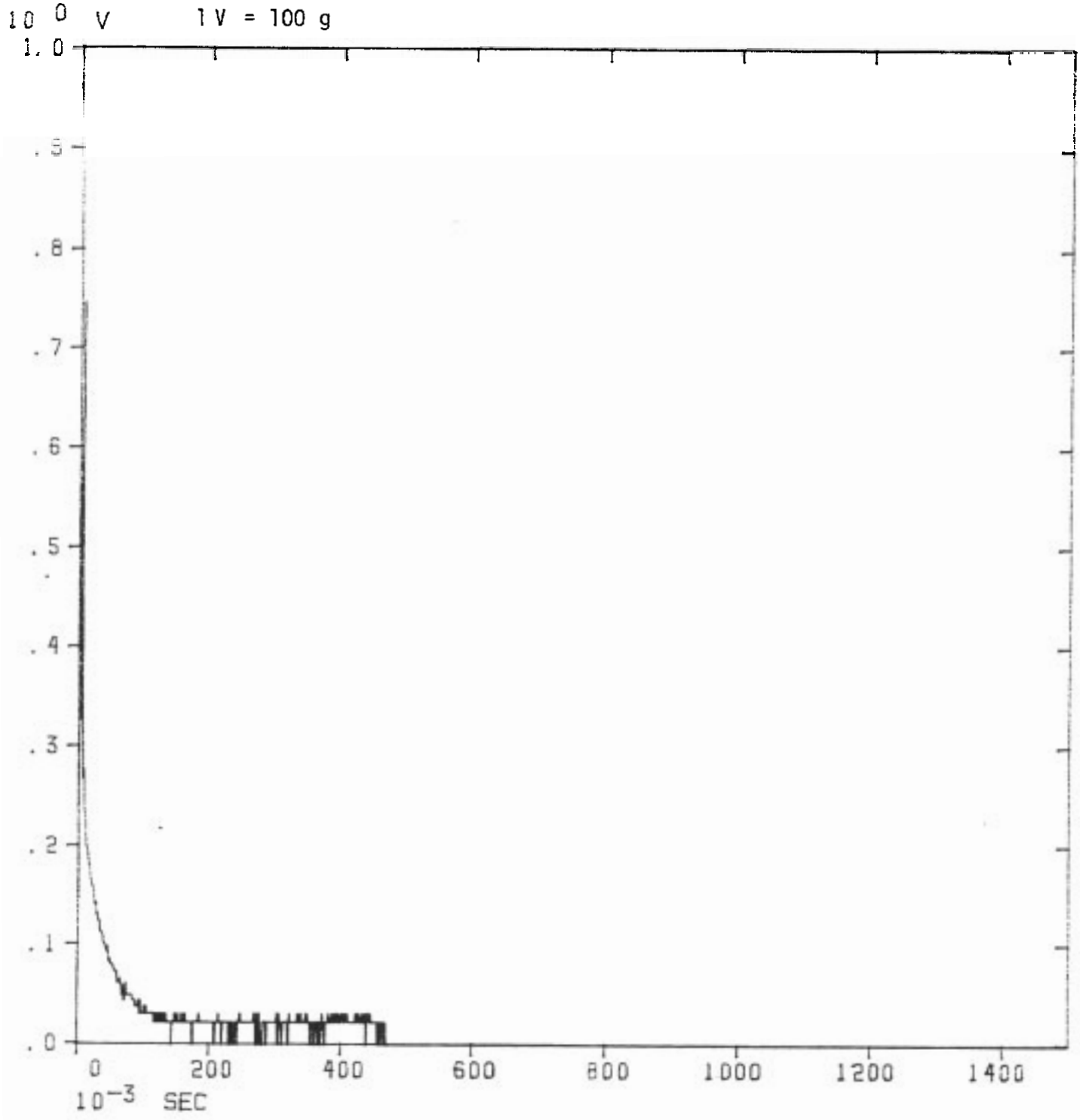

FIGURE D7 - Resultant knee acceleration for HZ Sedan with an aluminium bull-bar

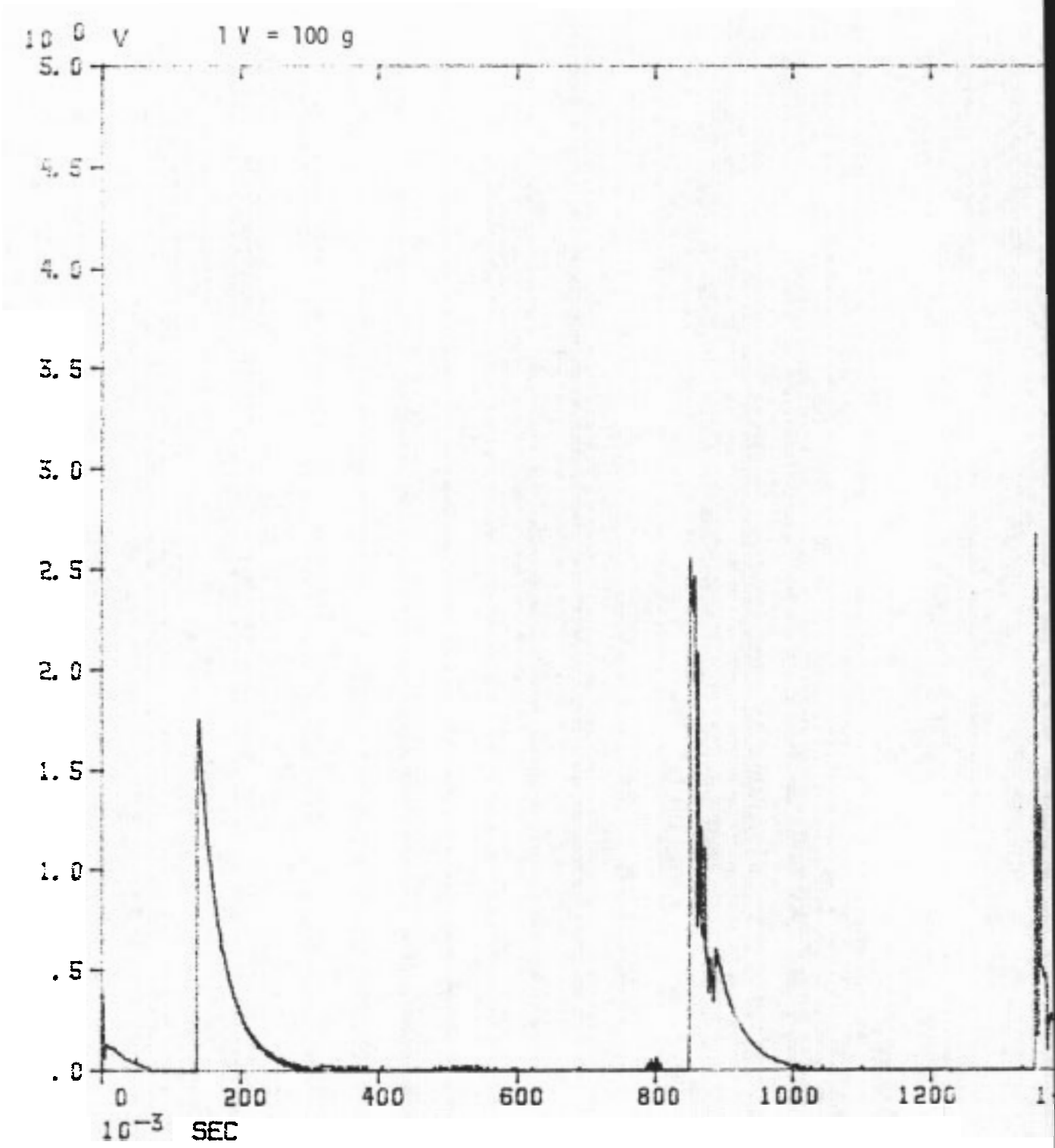

FIGURE D8 - Resultant knee acceleration for HZ Sedan with a tubular steel bull-bar

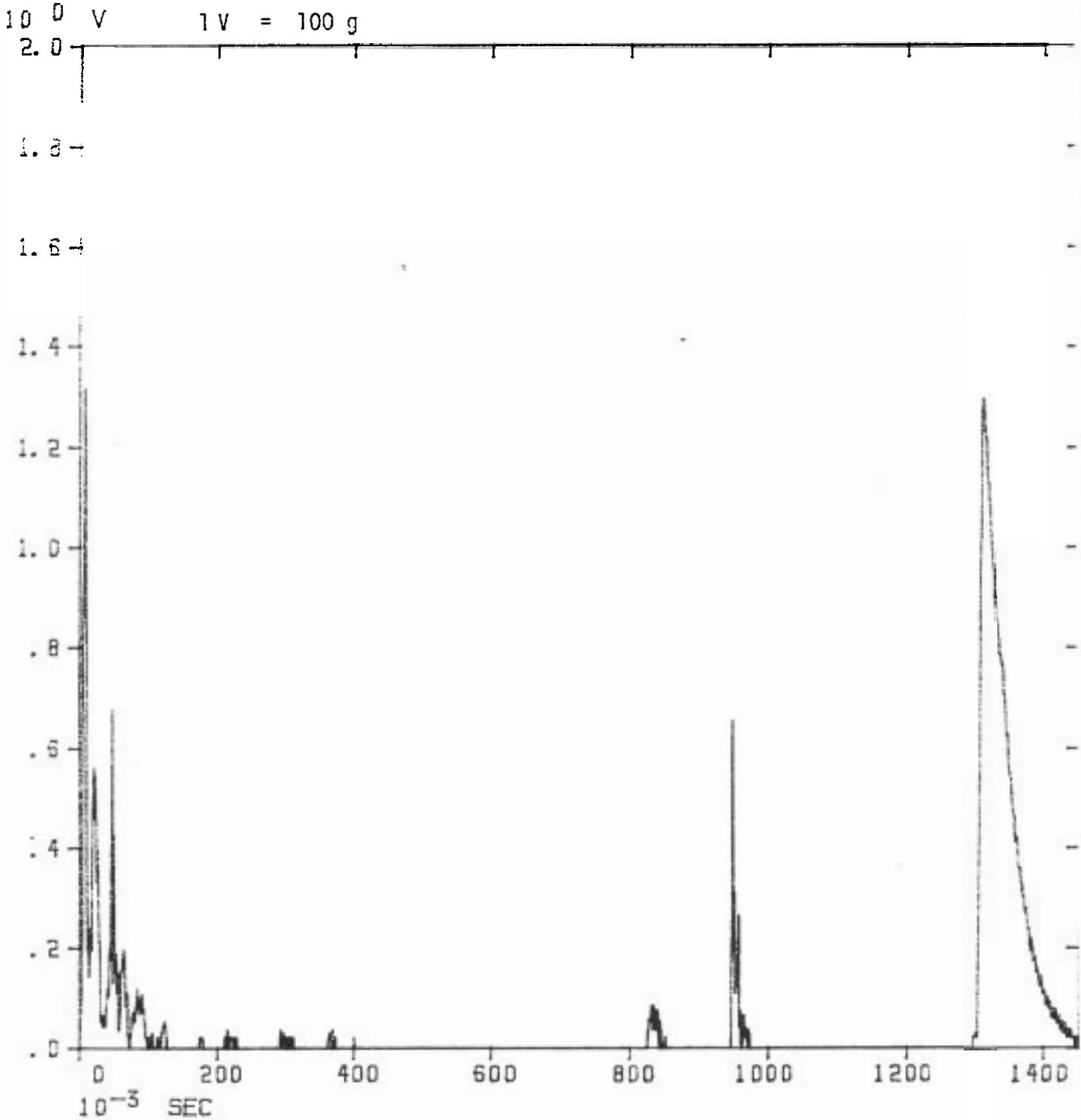

FIGURE D9 - Resultant knee acceleration for HZ Sedan with a truck type bull-bar

Secondary peaks on Figure D8 and D9 correspond to the harsh impact when the dummy was hitting the road and overturning on the back.

Pelvis (Fig. D10 - D13)

Pelvic accelerations during the primary impact were negligible. Secondary peaks were about 300 g in all cases but of a very short duration. **This indicates that there would be no pelvis injuries** in accidents at speeds of 20 km/hr.

Foot (Fig. D14 - D15)

Only two records are available. Fig. D13 shows foot acceleration in lateral direction for the impact with car without bull-bar. It shows that there was an impact on the lower leg and that after 100 ms the foot was free. **On the other hand, the aluminium bar loc** the foot between bar and road.

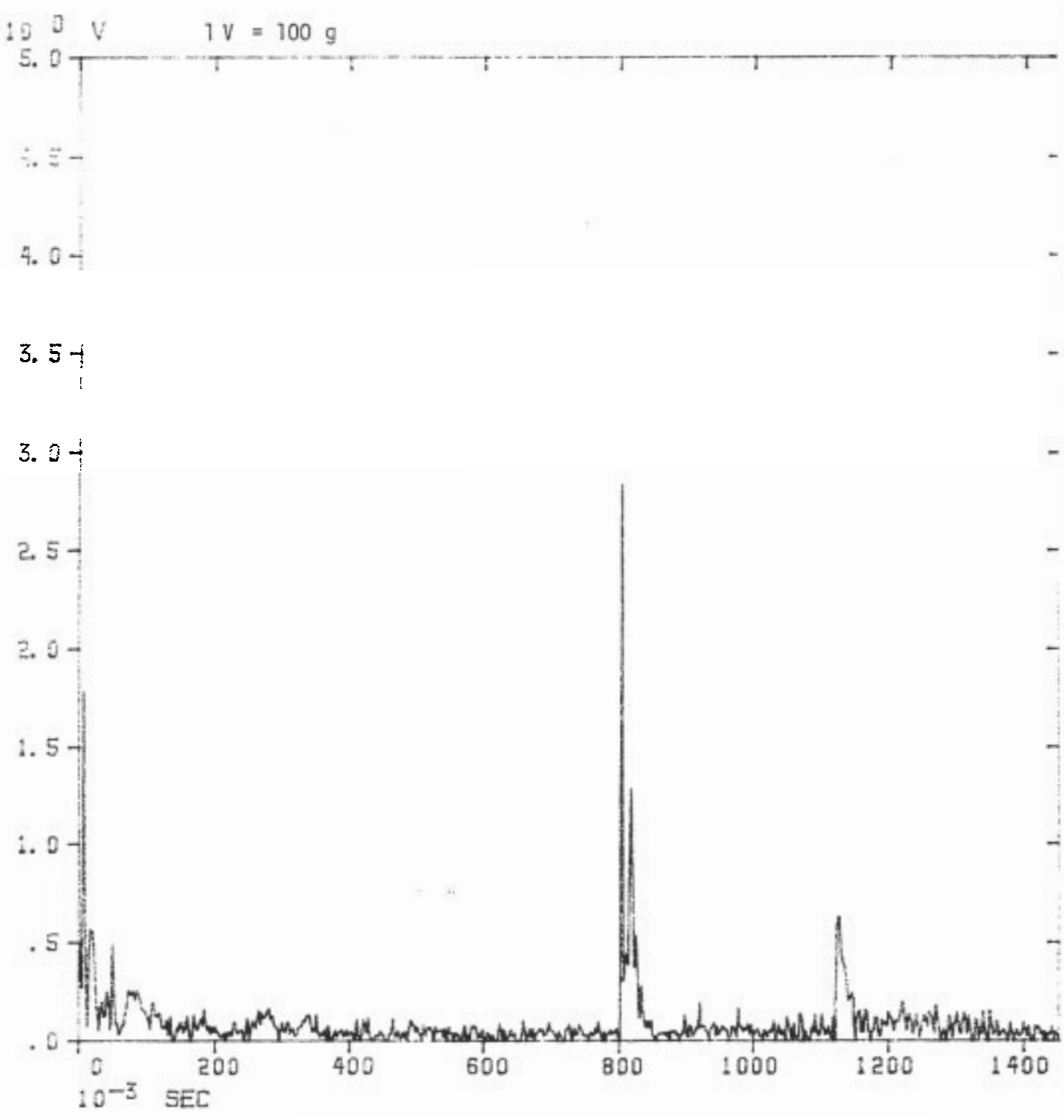

FIGURE D10 - Resultant pelvis acceleration for HZ Sedan without a bull-bar

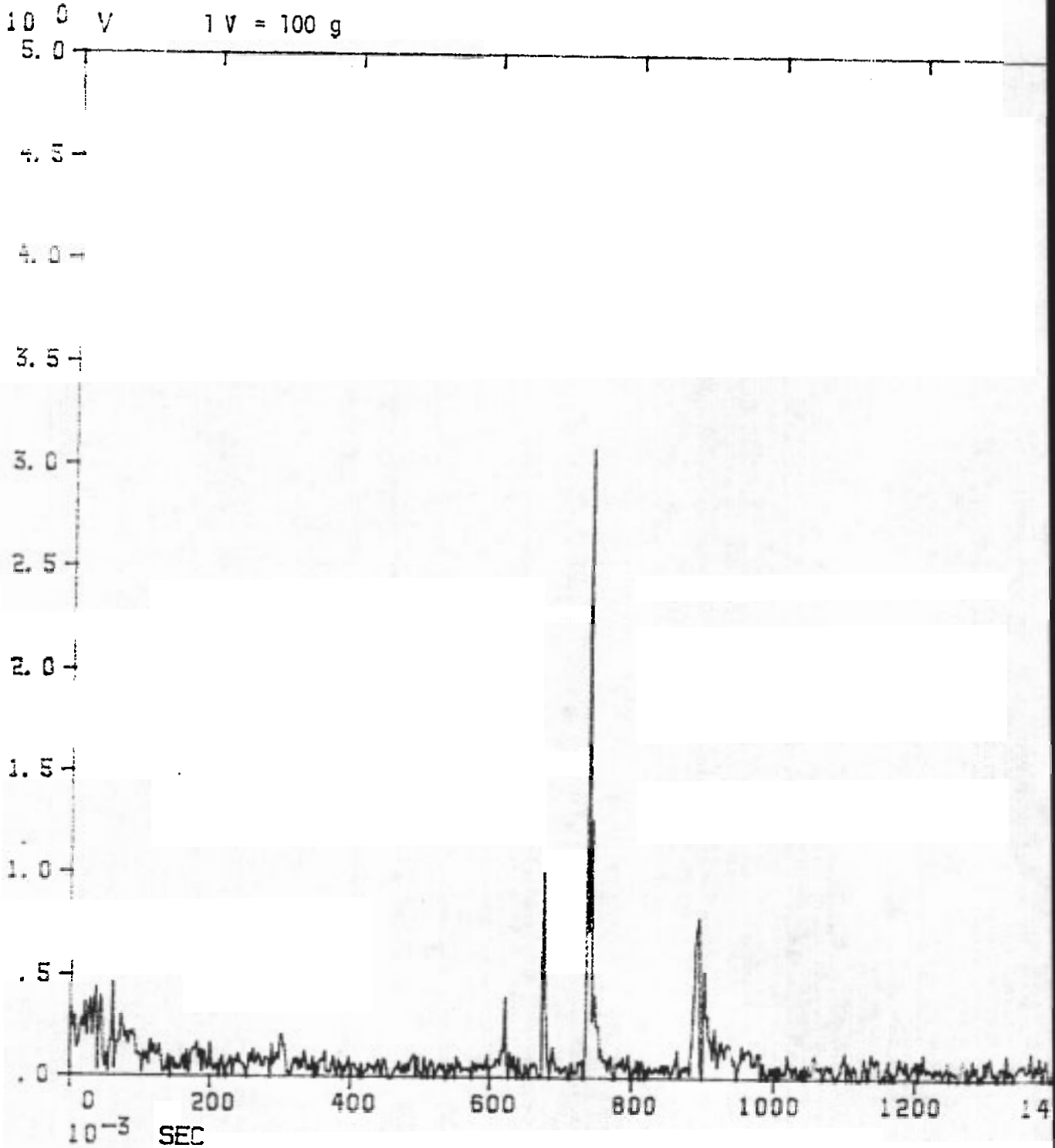

FIGURE D11 - Resultant pelvis acceleration for HZ Sedan with an aluminium bull-bar

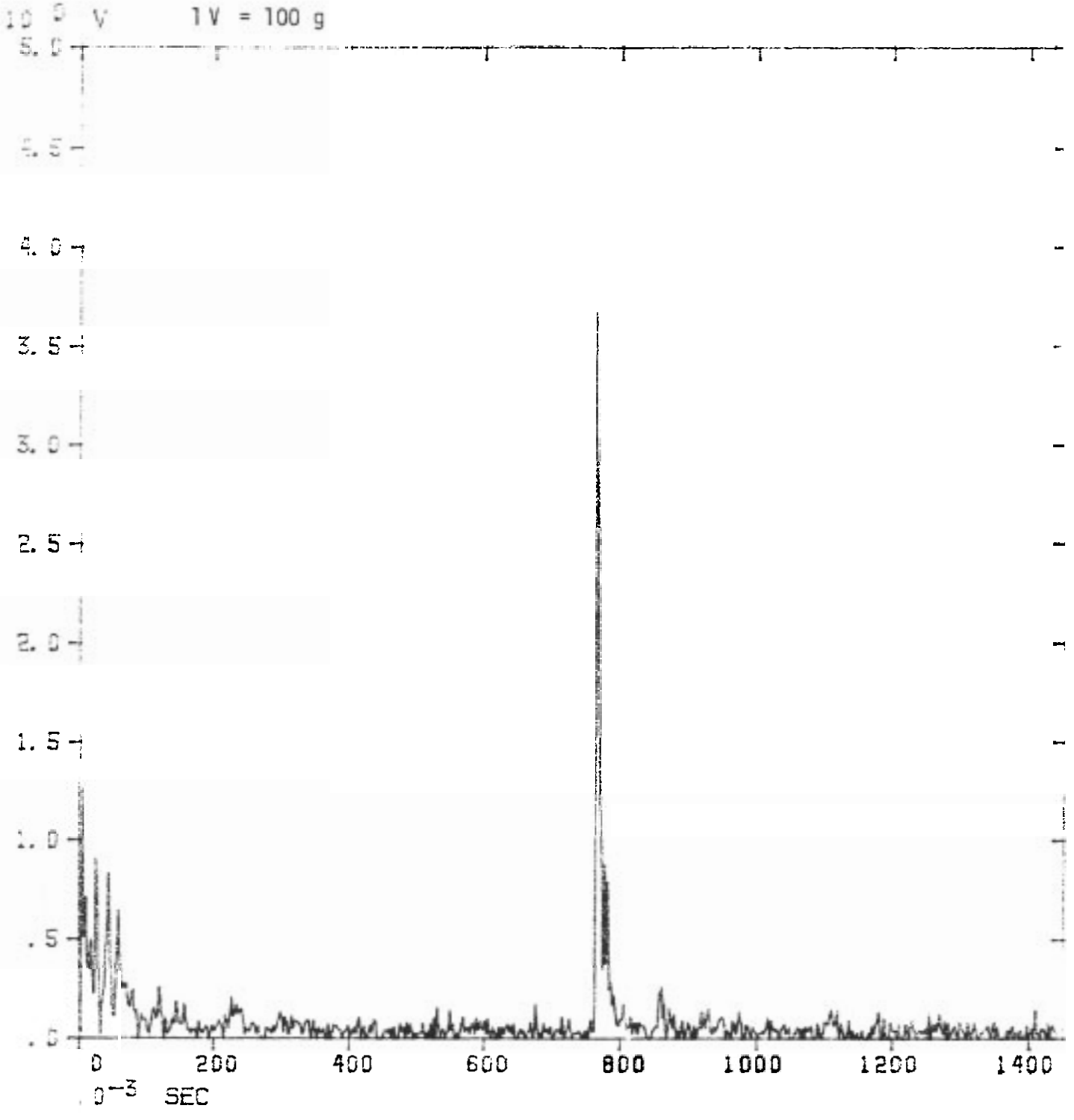

FIGURE D1 - Resultant pelvis acceleration for HZ Sedan with a tubular steel bull-bar

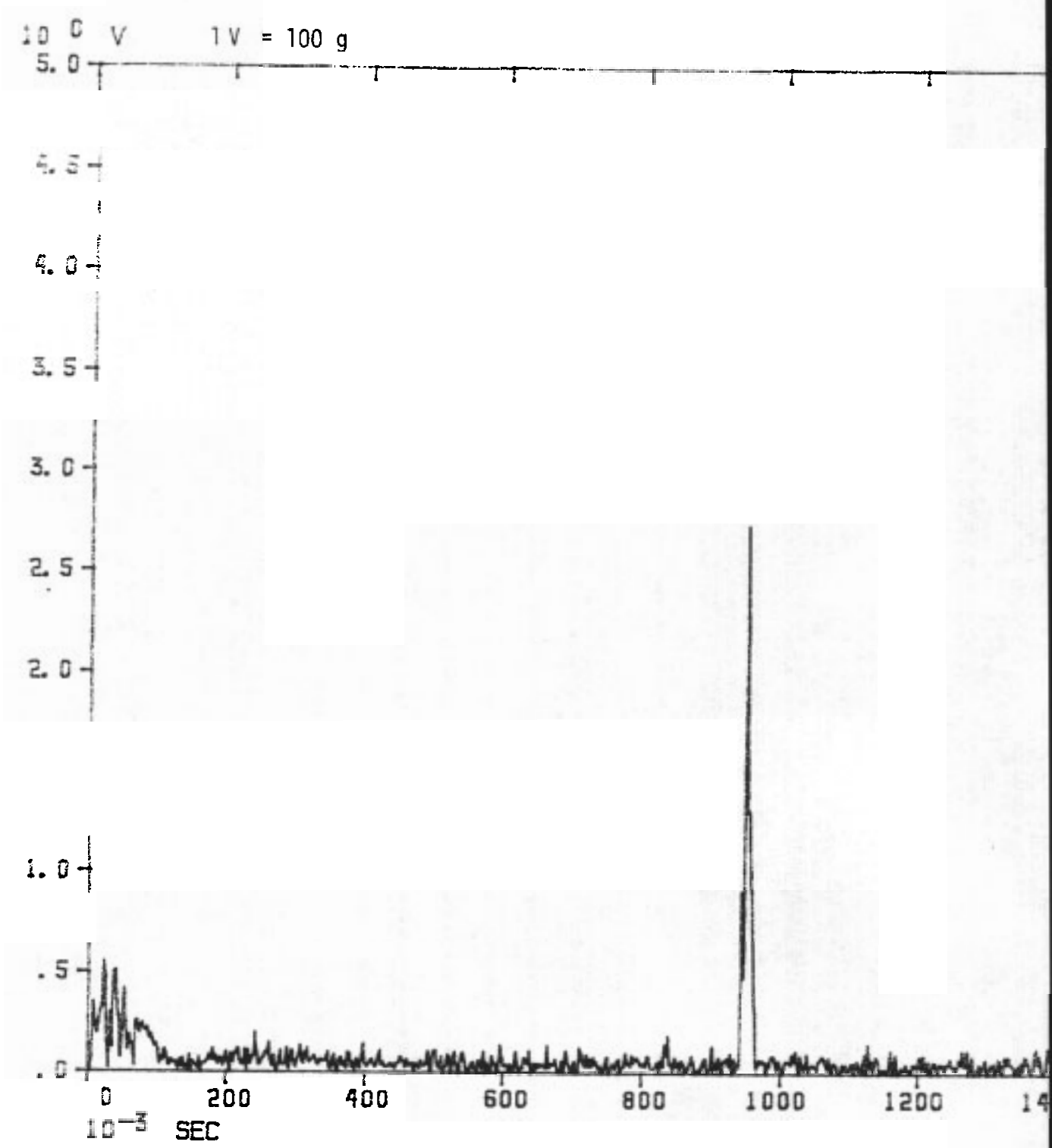

FIGURE D13 - Resultant pelvis acceleration for HZ Sedan with a touch-type bull-bar

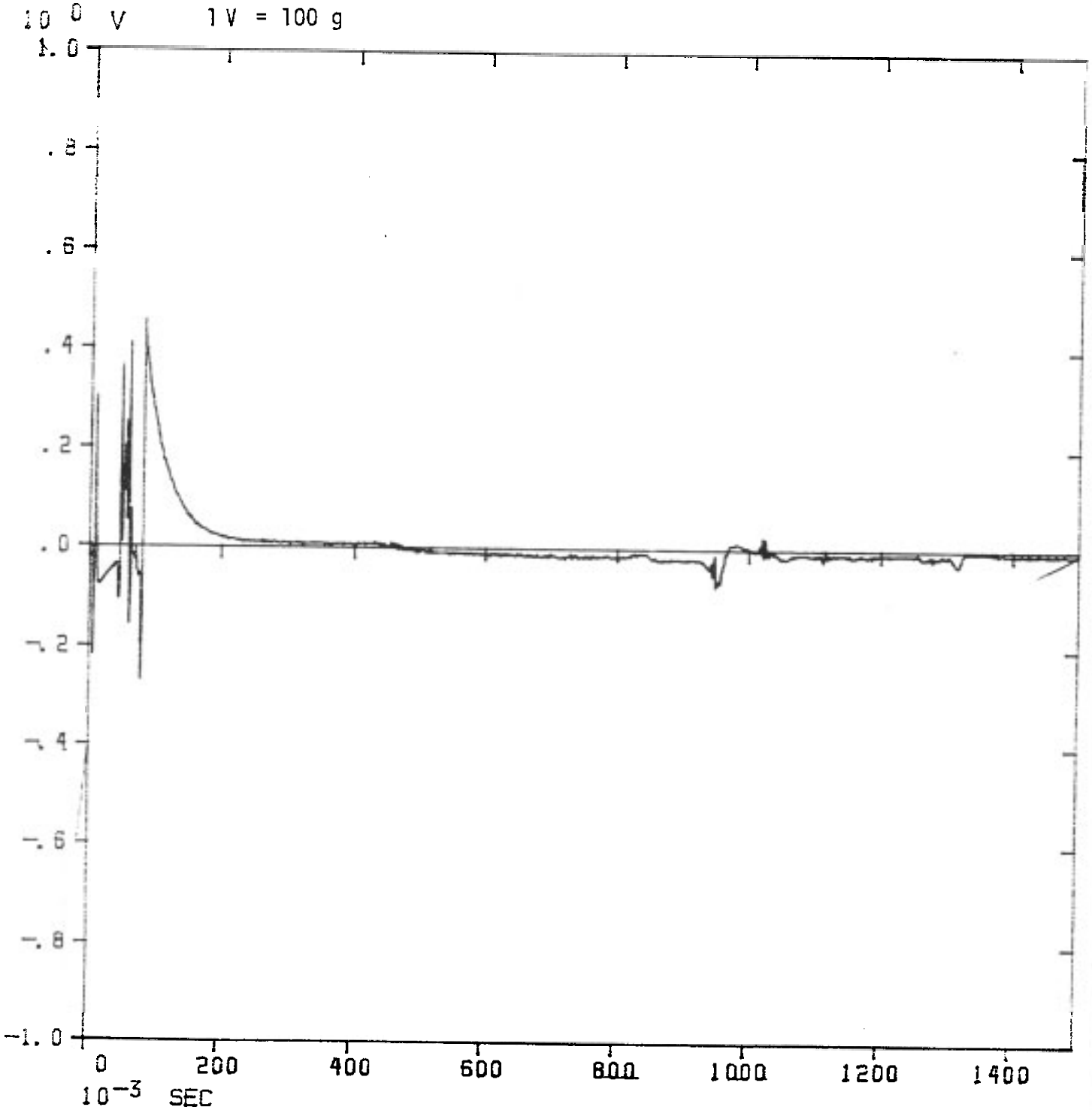

FIGURE D14 - Lateral acceleration of the foot for HZ Sedan without a bull-bar

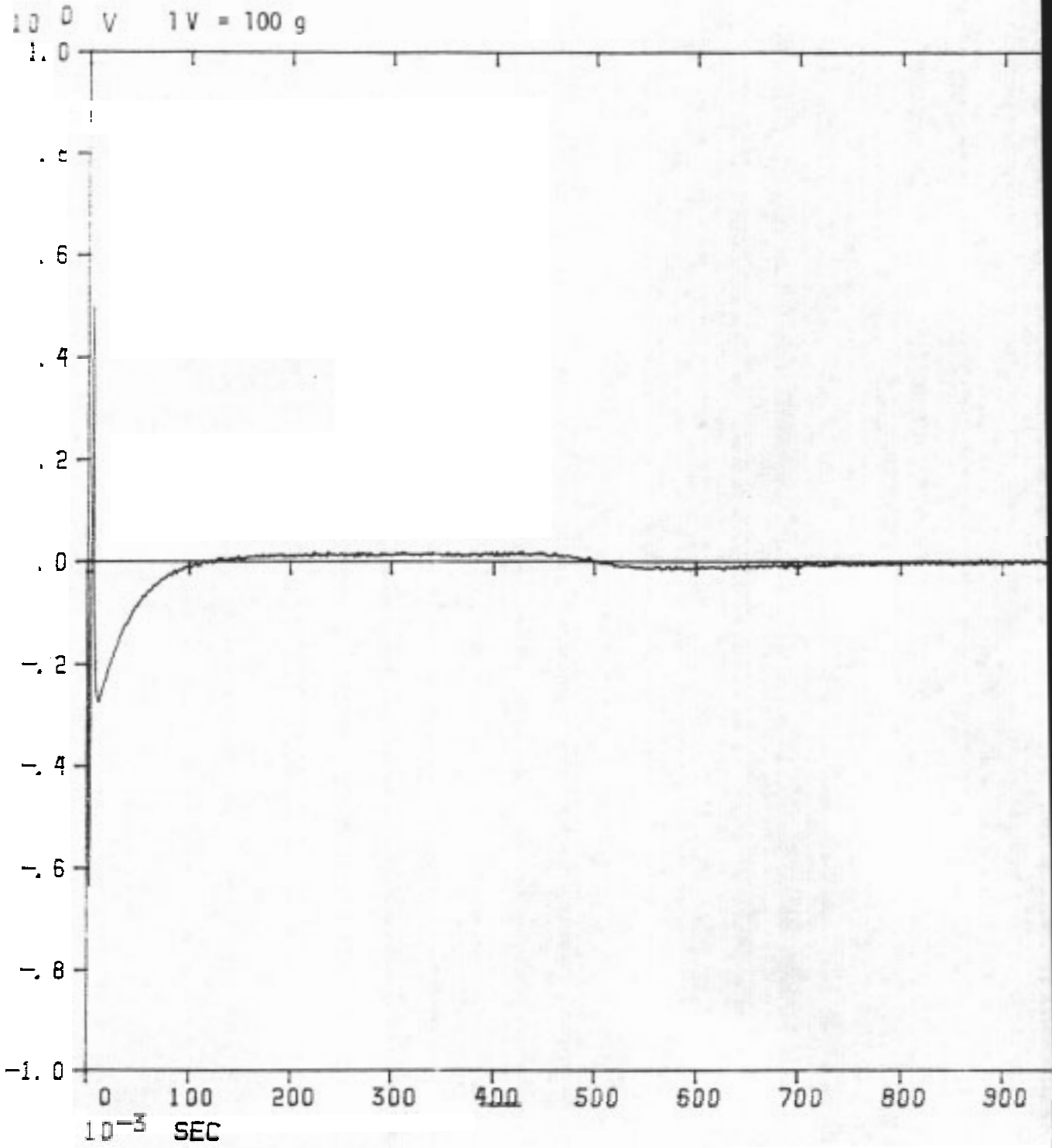

FIGURE D15 - Lateral acceleration of the foot for HZ Sedan with an aluminium bull-bar